

Confidence-Aware Imitation Learning from Demonstrations with Varying Optimality

Songyuan Zhang^{1*}, Zhangjie Cao^{2*}, Dorsa Sadigh², Yanan Sui¹

¹National Engineering Lab for Neuromodulation, SAE, Tsinghua University, China

²Department of Computer Science, Stanford University, USA

szhang21@mit.edu, {caozj, dorsa}@cs.stanford.edu, ysui@tsinghua.edu.cn

Abstract

Most existing imitation learning approaches assume the demonstrations are drawn from experts who are optimal, but relaxing this assumption enables us to use a wider range of data. Standard imitation learning may learn a suboptimal policy from demonstrations with varying optimality. Prior works use confidence scores or rankings to capture beneficial information from demonstrations with varying optimality, but they suffer from many limitations, *e.g.*, manually annotated confidence scores or high average optimality of demonstrations. In this paper, we propose a general framework to learn from demonstrations with varying optimality that jointly learns the confidence score and a well-performing policy. Our approach, Confidence-Aware Imitation Learning (CAIL) learns a well-performing policy from confidence-reweighted demonstrations, while using an outer loss to track the performance of our model and to learn the confidence. We provide theoretical guarantees on the convergence of CAIL and evaluate its performance in both simulated and real robot experiments. Our results show that CAIL significantly outperforms other imitation learning methods from demonstrations with varying optimality. We further show that even without access to any optimal demonstrations, CAIL can still learn a successful policy, and outperforms prior work.

1 Introduction

We consider an imitation learning setting that learns a well-performing policy from a mixture of demonstrations with varying optimality ranging from random trajectories to optimal demonstrations. As opposed to standard imitation learning, where the demonstrations come from experts and thus are optimal, this benefits from a larger and more diverse source of data. Note that different from setting that the demonstrations are optimal but lack some causal factors [32], in our setting, the demonstrations can be suboptimal. However, this introduces a new set of challenges. First, one needs to select useful demonstrations beyond the optimal ones. We are interested in settings where we do not have sufficient expert demonstrations in the mixture so we have to rely on learning from sub-optimal demonstrations that can still be successful at parts of the task. Second, we need to be able to filter the negative effects of useless or even malicious demonstrations, *e.g.*, demonstrations that implicitly fail the tasks.

To address the above challenges, we propose to use a measure of *confidence* to indicate the likelihood that a demonstration is optimal. A confidence score can provide a fine-grained characterization of each demonstration’s optimality. For example, it can differentiate between near-optimal demonstrations or adversarial ones. By reweighting demonstrations with a confidence score, we can simultaneously learn from useful but sub-optimal demonstrations while avoiding the negative effects of malicious ones. So

*Equal contribution.

our problem reduces to learning an accurate confidence measure for demonstrations. Previous work learns the confidence from manually annotated demonstrations [31], which are difficult to obtain and might contain bias—For example, a conservative and careful demonstrator may assign lower confidence compared to an optimistic demonstrator to the same demonstration. In this paper, we remove restrictive assumptions on the confidence, and propose an approach that automatically learns the confidence score for each demonstration based on evaluation of the outcome of imitation learning. This evaluation often requires access to limited *evaluation data*.

We propose a new algorithm, Confidence-Aware Imitation Learning (CAIL), to jointly learn a well-performing policy and the confidence for every state-action pair in the demonstrations. Specifically, our method adopts a standard imitation learning algorithm and evaluates its performance to update the confidence scores with an evaluation loss, which we refer to as the *outer loss*. In our implementation, we use a limited amount of ranked demonstrations as our evaluation data for the outer loss. We then update the policy parameters using the loss of the imitation learning algorithm over the demonstrations reweighted by the confidence, which we refer to as the *inner loss*. Our framework can accommodate any imitation learning algorithm accompanied with an evaluation loss to assess the learned policy.

We optimize for the inner and outer loss using a bi-level optimization [5], and prove that our algorithm converges to the optimal confidence assignments under mild assumptions. We further implement the framework using Adversarial Inverse Reinforcement Learning (AIRL) [14] as the underlying imitation learning algorithm along with its corresponding learning loss as our inner loss. We design a ranking loss as the outer loss, which is compatible with the AIRL model and only requires easy-to-access ranking annotations rather than the exact confidence values.

The main contributions of the paper can be summarized as:

- We propose a novel framework, Confidence-Aware Imitation Learning (CAIL), that jointly learns confidence scores and a well-performing policy from demonstrations with varying optimality.
- We formulate our problem as a modified bi-level optimization with a pseudo-update step and prove that the confidence learned by CAIL converges to the optimal confidence in $\mathcal{O}(1/\sqrt{T})$ (T is the number of steps) under some mild assumptions.
- We conduct experiments on several simulation and robot environments. Our results suggest that the learned confidence can accurately characterize the optimality of demonstrations, and that the learned policy achieves higher expected return compared to other imitation learning approaches.

2 Related Work

Imitation Learning. The most common approaches for imitation learning are Behavioral Cloning (BC) [21, 4, 24, 23, 3], which treats the problem as a supervised learning problem, and Inverse Reinforcement Learning (IRL), which recovers the reward function from expert demonstrations and finds the optimal policy through reinforcement learning over the learned reward [1, 22, 33]. More recently, Generative Adversarial Imitation Learning (GAIL) [18] learns the policy by matching the occupancy measure between demonstrations and the policy in an adversarial manner [15]. Adversarial Inverse Reinforcement Learning (AIRL) [14] and some other approaches [13, 17] improve upon GAIL by simultaneously learning the reward function, and the optimal policy. However, these approaches assume that all the demonstrations are expert demonstrations, and cannot learn a well-performing policy when learning from demonstrations with varying optimality.

Learning from Demonstrations with Varying Optimality: Ranking-based. Ranking-based methods learn a policy from a sequence of demonstrations annotated with rankings [2, 26, 30, 10]. T-REX learns a reward from the ranking of the demonstrations and learns a policy using reinforcement learning [8]. In our work, we assume access to rankings of a small subset of the demonstrations. The reward function learned from such a small number of rankings by T-REX may have low generalization ability to out of distribution states. D-REX improves T-REX by automatically generating the rankings of demonstrations [9], and SSRR further finds the structure of the reward function [12]. These techniques automatically generate rankings under the assumption that a perturbed demonstration will have a lower reward than the original demonstration, which is not necessarily true for random or malicious demonstrations that can be present in our mixture. DPS utilizes partial orders and pairwise comparisons over trajectories to learn and generate new policies [19]. However, it requires interactively collecting feedback, which is not feasible in our offline learning setting.

Learning from Demonstrations with Varying Optimality: Confidence-based. Confidence-based methods assume each demonstration or demonstrator holds a confidence value indicating their optimality and then reweight the demonstrations based on this value for imitation learning. To learn the confidence, 2IWIL requires access to ground-truth confidence values for the demonstrations to accurately learn a confidence predictor [31]. Tangkaratt *et al.* require that all the actions for a demonstration are drawn from the same noisy distribution with sufficiently small variance [28]. IC-GAIL implicitly learns the confidence score by aligning the occupancy measure of the learned policy with the expert policy, but requires a set of ground-truth labels to estimate the average confidence [31]. Following works relax the assumption of access to the ground-truth confidence, but still require more optimal demonstrations than non-optimal ones in the dataset [27]. Other works require access to the reward of each demonstration [11]. All of these methods either rely on a specific imitation learning algorithm or require strong assumptions on the confidence. To move forward, we propose a general framework to jointly learn the confidence and the policy. Our framework is flexible as it can use any imitation learning algorithm as long as there exists a compatible outer loss, *i.e.*, the outer loss can evaluate the quality of the imitation learning model.

3 Problem Setting

We formulate the problem of learning from demonstrations with varying optimality as a Markov decision process (MDP): $\mathcal{M} = \langle \mathcal{S}, \mathcal{A}, \mathcal{T}, \mathcal{R}, \rho_0, \gamma \rangle$, where \mathcal{S} is the state space, \mathcal{A} is the action space, $\mathcal{T} : \mathcal{S} \times \mathcal{A} \times \mathcal{S} \rightarrow [0, 1]$ is the transition probability, ρ_0 is the distribution of initial states, $\mathcal{R} : \mathcal{S} \times \mathcal{A} \rightarrow \mathbb{R}$ is the reward function, and γ is the discount factor. A policy $\pi : \mathcal{S} \times \mathcal{A} \rightarrow [0, 1]$ defines a probability distribution over the action space in a given state. The expected return, which evaluates the quality of a policy, can be defined as $\eta_\pi = \mathbb{E}_{s_0 \sim \rho_0, \pi} [\sum_{t=0}^{\infty} \gamma^t \mathcal{R}(s_t, a_t)]$, where t indicates the time step.

We aim to learn a policy that imitates the behavior of a demonstrator d following policy π^d who provides a set of demonstrations $\Xi = \{\xi_1, \dots, \xi_D\}$ and $\xi_i \sim \pi^d$. Each trajectory is a sequence of state-action pairs $\xi = \{s_0, a_0, \dots, s_N\}$, and the expected return of a trajectory is $\eta_\xi = \sum_{t=0}^{N-1} \gamma^t \mathcal{R}(s_t, a_t)$.

A common assumption in classical imitation learning work is that the demonstrations are drawn from the expert policy $\pi^d = \pi^*$, *i.e.*, the policy that optimizes the expected return of the MDP \mathcal{M} [18, 14]. Here, we relax this assumption so that the demonstrations may contain non-expert demonstrations or even failures—drawn from policies other than π^* . Given the demonstration set \mathcal{D} , we need to assess our *confidence* in each demonstration. To achieve learning confidence over this mixture of demonstrations, we rely on the ability to evaluate the performance of imitation learning. This can be achieved by using an evaluation loss trained on *evaluation data*, \mathcal{D}_E (as shown in Fig. 1). In our implementation, we rely on a small amount of rankings between trajectories as our evaluation data: $\mathcal{D}_E = \eta_{\xi_1} \geq \dots \geq \eta_{\xi_m}$. To summarize, our framework takes a set of demonstrations with varying optimality \mathcal{D} as well as a limited amount of evaluation data \mathcal{D}_E along with an evaluation loss to find a well-performing policy. Note that unlike prior work [31], we do not assume that optimal demonstrations always exist in the demonstration set, and CAIL can still extract useful information from \mathcal{D} while avoiding negative effects of non-optimal demonstrations.

4 Confidence-Aware Imitation Learning

In our framework, we adopt an imitation learning algorithm with a model F_θ parameterized by θ and a corresponding imitation learning loss \mathcal{L}_{in} , which we refer to as inner loss (as shown in Figure 1). We assign each state-action pair a confidence value indicating the likelihood of the state-action pair appearing in the well-performing policy. The confidence can be defined as a function mapping from a state-action pair to a scalar value $\beta : \mathcal{S} \times \mathcal{A} \rightarrow \mathbb{R}$. We aim to find the optimal confidence assignments β^* to reweight state-action pairs within the demonstrations. We then conduct imitation learning from the reweighted demonstrations using the inner imitation loss \mathcal{L}_{in} to learn a well-performing policy. Here, we first define the optimal confidence β^* and describe how to learn it automatically.

Defining the Optimal Confidence. We define the distribution of state-action pairs visited by a policy π based on the occupancy measure $\rho_\pi : \mathcal{S} \times \mathcal{A} \rightarrow \mathbb{R}$: $\rho_\pi(s, a) = \pi(a|s) \sum_{t=0}^{\infty} \gamma^t P(s_t = s|\pi)$, which can be explained as the un-normalized distribution of state transitions that an agent encounters when navigating the environment with the policy π . We can normalize the occupancy measure to form the

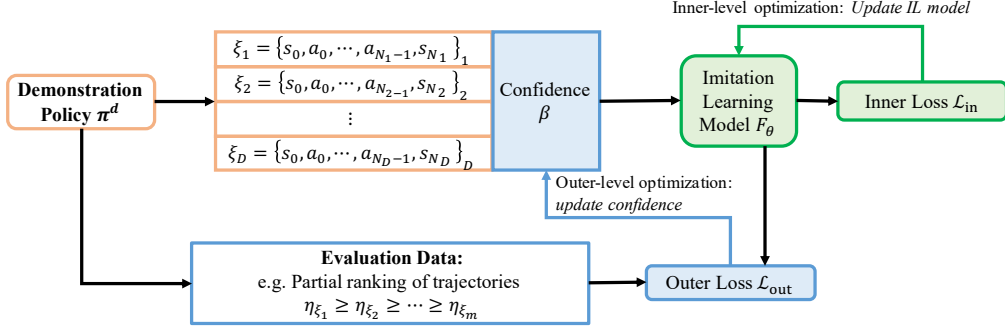


Figure 1: Confidence-Aware Imitation Learning. The demonstrations are shown in the orange box drawn from demonstration policy: $\xi_1, \dots, \xi_D \sim \pi^d$. The confidence learning component and the outer loss are shown in blue. The confidence β reweights the distribution of state-action pairs in the demonstration set, and then the imitation learning model F_θ learns a well-performing policy and new parameters θ with the confidence-reweighted distribution using the inner loss (imitation loss) shown in green. Next iteration, the updated F_θ generates new trajectories that are then evaluated by the outer loss and potentially other evaluation data (e.g. partial ranking of trajectories) to update confidence.

state-action distribution: $p_\pi(s, a) = \frac{\rho_\pi(s, a)}{\sum_{s, a} \rho_\pi(s, a)}$. Recall that π^d is the policy that the demonstrations are derived from, which can potentially be a mixture of different expert, suboptimal, or even malicious policies. We reweight the state-action distribution of the demonstrations to derive a new state-action distribution, which corresponds to another policy π_{new} : $p_{\pi_{\text{new}}}(s, a) = \beta(s, a)p_{\pi^d}(s, a)$. Our goal is to find the optimal confidence β^* that ensures the derived policy π_{new} maximizes the expected return:

$$\beta^*(s, a) = \arg \max_{\beta} \eta_{\pi_{\text{new}}}. \quad (1)$$

With such $\beta^*(s, a)$, we can conduct imitation learning from the reweighted demonstrations to maximize the expected return with the provided demonstrations.

Learning the Confidence. We will learn an estimate of the confidence score β without access to any annotations of the ground-truth values based on optimizing two loss functions: The inner loss and the outer loss. The inner loss \mathcal{L}_{in} is accompanied by the imitation learning algorithm encouraging imitation, while the outer loss \mathcal{L}_{out} captures the quality of imitation learning, and thus optimizing it finds the confidence value that maximizes the performance of the imitation learning algorithm. Specifically, we first learn the imitation learning model parameters θ^* that minimize the inner loss:

$$\theta^*(\beta) = \arg \min_{\theta} \mathbb{E}_{(s, a) \sim \beta(s, a)p_{\pi^d}(s, a)} \mathcal{L}_{\text{in}}(s, a; \theta, \beta) \quad (2)$$

We note that the inner loss $\mathcal{L}_{\text{in}}(s, a; \theta, \beta)$ refers to settings where (s, a) is sampled from the distribution $\beta(s, a)p_{\pi^d}(s, a)$, and hence implicitly depends on β . Thus we need to find the optimal β^* , which can be estimated by minimizing an outer loss \mathcal{L}_{out} :

$$\beta_{\text{out}}^* = \arg \min_{\beta} \mathcal{L}_{\text{out}}(\theta^*(\beta)). \quad (3)$$

This evaluates the performance of the underlying imitation learning algorithm with respect to the reward with limited evaluation data \mathcal{D}_E (e.g. limited rankings if we select a ranking loss as our choice of \mathcal{L}_{out} ; which we will discuss in detail in Sec. 4.3).

4.1 Optimization of Outer and Inner Loss

We design a bi-level optimization process consisting of an inner-level optimization and an outer-level optimization to simultaneously update the confidence β and the model parameters θ . Within the outer-level optimization, we first pseudo-update the imitation learning parameters to build a connection between β and the optimized parameters θ' with the current β . We then update β to make the induced θ' minimize the outer loss \mathcal{L}_{out} in Eqn. (3). The inner-level optimization is to find the imitation learning model parameters that minimize inner loss \mathcal{L}_{in} with respect to the confidence β . We introduce the details of the optimization below. We use τ to denote the number of iterations. Note that the losses in this section are all computed based on the expectation over states and actions.

Outer-Level Optimization: Updating β . Let β_τ be the confidence at time τ . Using β_τ , we first pseudo-update the imitation learning parameters θ using gradient descent. Here pseudo-update means that the update aims to compute the gradients of β but does not really change the value of θ . Let $\theta'_0 = \theta_\tau$ be the current imitation learning model parameters, and we update θ' as:

$$\theta'_{t+1} = \theta'_t - \mu \nabla_{\theta'} \mathcal{L}_{\text{in}}(s, a; \theta'_t, \beta_\tau), \quad (4)$$

where μ is the learning rate, t is the pseudo-updating time step for θ' . We will update θ' with respect to the fixed β_τ after convergence of Eqn. (4). After updating θ' , we now update β using gradient descent with the outer loss \mathcal{L}_{out} from Eqn. (3):

$$\beta_{\tau+1} = \beta_\tau - \alpha \nabla_\beta \mathcal{L}_{\text{out}}(\theta'), \quad (5)$$

where α is the learning rate for updating β . Intuitively, updating β as in Eqn. (5) aims to find the fastest update direction of θ' for decreasing the outer loss \mathcal{L}_{out} . Though we compute gradients of gradients for β here, β is only a one-dimension scalar for each state-action pair and within each iteration of training, we only sample a mini-batch of thousands of state-pairs for update. Thus, within each iteration, the total dimension of β is small and computing the gradient of gradient is not costly.

Inner-Level Optimization: Updating θ . With the updated $\beta_{\tau+1}$, we now will update θ using gradient descent, where we denote the initialization as $\theta_0 = \theta_\tau$.

$$\theta_{t+1} = \theta_t - \mu \nabla_\theta \mathcal{L}_{\text{in}}(s, a; \theta_t, \beta_{\tau+1}). \quad (6)$$

After convergence, we set $\theta_{\tau+1} = \theta$. With the two updates introduced above (outer and inner optimization), we finish one update iteration with setting β_τ to $\beta_{\tau+1}$ using the converged value from Eqn. (5) and θ_τ to $\theta_{\tau+1}$ using the converged value from Eqn. (6).

In each iteration of the above optimization—in the steps of pseudo-updating and the steps of updating the imitation learning model—multiple gradient steps are required for convergence, meaning that there is a nested loop of gradient descent algorithms. The nested loop costs quadratic time and is inefficient especially for deep networks. To further accelerate the optimization, we propose an approximation, which only updates θ once in the pseudo-updating and the updating steps. Therefore, the new updating rule can be formalized as follows:

$$\begin{aligned} \theta'_{\tau+1} &= \theta_\tau - \mu \nabla_{\theta'} \mathcal{L}_{\text{in}}(s, a; \theta_\tau, \beta_\tau), \\ \beta_{\tau+1} &= \beta_\tau - \alpha \nabla_\beta \mathcal{L}_{\text{out}}(\theta'_{\tau+1}), \\ \theta_{\tau+1} &= \theta_\tau - \mu \nabla_\theta \mathcal{L}_{\text{in}}(s, a; \theta_\tau, \beta_{\tau+1}). \end{aligned} \quad (7)$$

4.2 Theoretical Results

We analyze the convergence of the proposed bi-level optimization algorithm for the CAIL framework and derive the following theorems. We provide the detailed proofs of these theorems in Appendix.

Theorem 1. (Convergence) Suppose the outer loss \mathcal{L}_{out} is Lipschitz-smooth with constant L , the inequality

$$\nabla_\theta \mathcal{L}_{\text{out}}(\theta_{\tau+1})^\top \nabla_\theta \mathcal{L}_{\text{in}}(\theta_\tau, \beta_{\tau+1}) \geq C \|\nabla_\theta \mathcal{L}_{\text{in}}(\theta_\tau, \beta_{\tau+1})\|^2 \quad (8)$$

holds for a constant $C \geq 0$ in every step τ ,² and the learning rate satisfies $\mu \leq \frac{2C}{L}$, then the outer loss decreases along with each iteration: $\mathcal{L}_{\text{out}}(\theta_{\tau+1}) \leq \mathcal{L}_{\text{out}}(\theta_\tau)$, and the equality holds if $\nabla_\beta \mathcal{L}_{\text{out}}(\theta_\tau) = 0$ or $\theta_{\tau+1} = \theta_\tau$.

Remark 1. The inequality in the assumption of Theorem 1 (Eqn. 8) indicates that the directions of the gradients of \mathcal{L}_{out} and \mathcal{L}_{in} with respect to θ should be close. Intuitively only when the two gradient directions align, we can decrease the evaluation loss \mathcal{L}_{out} by updating θ with \mathcal{L}_{in} .

Theorem 1 ensures that the confidence and the imitation learning parameters monotonically decrease the outer loss. When the gradient of the outer loss with respect to β is zero, β converges to the optimal confidence that minimizes the outer loss, i.e., β^* in Eqn. (1). With the optimal confidence, we can learn a well-performing policy from more useful demonstrations by reweighting them. Thus, the learned imitation model induces lower outer loss (has higher-quality) than the imitation learning model learned from the original demonstrations in the dataset without reweighting.

²We remove (s, a) in \mathcal{L}_{in} for notation simplicity.

Theorem 2. (Convergence Rate) Under the assumptions in Theorem 1, let

$$g(\theta, \beta) = \theta - \mu \nabla_{\theta} \mathcal{L}_{in}(s, a; \theta, \beta) \quad (9)$$

We assume that $\mathcal{L}_{out}(g(\theta, \beta))$ is Lipschitz-smooth w.r.t. β with constant L_1 , \mathcal{L}_{in} and \mathcal{L}_{out} have σ -bounded gradients, and the norm of $\nabla_{\beta} \nabla_{\theta} \mathcal{L}_{in}(\theta; \beta)$ is bounded by σ_1 . L is the Lipschitz-smooth constant for \mathcal{L}_{out} w.r.t. $g(\theta, \beta)$ as shown in Theorem 1. Consider the total training steps as T , we set $\alpha = \frac{C_1}{\sqrt{T}}$, for some constant C_1 where $0 < C_1 \leq \frac{2}{L_1}$ and $\mu = \frac{C_2}{T}$ for some constant C_2 . Then:

$$\min_{1 \leq \tau \leq T} \mathbb{E}[\|\nabla_{\beta} \mathcal{L}_{out}(\theta_{\tau})\|^2] \leq O\left(\frac{1}{\sqrt{T}}\right). \quad (10)$$

Remark 2. The assumptions of Theorem 2 are Lipschitz-smoothness and bounded first-order and second-order gradients of \mathcal{L}_{in} and \mathcal{L}_{out} , which are satisfied for typical \mathcal{L}_{in} and \mathcal{L}_{out} such as the cross-entropy loss of AIRL and the ranking loss in our implementation of CAIL in Section 4.3.

With the bound on the convergence rate, the gradient of the outer loss with respect to β is gradually getting close to 0, which means that β gradually converges to the optimal confidence β^* that minimizes the outer loss if \mathcal{L}_{out} is convex with respect to β .

4.3 An Implementation of CAIL

To implement CAIL, we need to adopt an imitation learning algorithm whose imitation loss will be the inner loss. We also need to design an outer loss on the imitation learning algorithm to evaluate the quality of imitation given some evaluation data \mathcal{D}_E (e.g. partial ranking annotations).

Based on the above considerations, as an instance of the implementation of CAIL, we use Adversarial Inverse Reinforcement Learning (AIRL) [14] as our imitation learning model. We use the imitation loss of AIRL as the inner loss, and a ranking loss (based on a partial ranking of trajectories) as the outer loss. AIRL and the ranking loss are compatible since AIRL can induce the reward function from the discriminator within the model, and the ranking loss can penalize the mismatches of the trajectory rankings computed by the induced reward function and the ground-truth rankings from the evaluation data \mathcal{D}_E . Furthermore, the implementation only requires the ranking of a subset of demonstrations $\{\xi_i\}_{i=1}^m \subset \Xi$, i.e., $\mathcal{D}_E = \eta_{\xi_1} \geq \eta_{\xi_2} \geq \dots \geq \eta_{\xi_m}$, which is much easier to access than the exact confidence value annotations [6, 19] since confidence not only reflects the rankings of different demonstrations but also how much one demonstration is better than the other.

AIRL consists of a generator G parameterized by θ_G as the policy, and a discriminator parameterized by θ_D . The generator and the discriminator are trained in an adversarial manner as in [15] to match the occupancy measures of the policy and the demonstrations. We write the loss \mathcal{L}_{in} as:

$$\mathcal{L}_{in}^D(s, a; \theta^D, \beta) = \mathbb{E}_{(s,a) \sim \beta(s,a)p_{\pi^d(s,a)}} [-\log D(s, a)] + \mathbb{E}_{(s,a) \sim \pi_{\theta_G}} [-\log(1 - D(s, a))], \quad (11)$$

$$\mathcal{L}_{in}^G(s, a; \theta^G) = \mathbb{E}_{(s,a) \sim \pi_{\theta_G}} [\log D(s, a) - \log(1 - D(s, a))], \quad (12)$$

where \mathcal{L}_{in}^D is the inner loss for the discriminator, \mathcal{L}_{in}^G is the inner loss for the generator and π_{θ_G} is the policy derived from the generator. The discriminator D is learned by minimizing the loss \mathcal{L}_{in}^D , which aims to discriminate the state-action pair (s, a) drawn from π_{θ_G} and the state-action pair (s, a) drawn from π^d . The generator parameter θ^G is trained to minimize the loss \mathcal{L}_{in}^G , which enables the generator to generate state-action pairs that are similar to the state transitions in the demonstrations.

For the outer loss, AIRL approximates the reward function by the discriminator parameters, i.e., \mathcal{R}'_{θ_D} . We compute $\eta'_{\xi_i} = \sum_{t=0}^N \gamma^t \mathcal{R}'_{\theta_D}(s_t, a_t)$ as the expected return of a trajectory using the reward \mathcal{R}'_{θ_D} . Then we penalize the mismatches of the rankings derived by η'_{ξ_i} and the ground-truth rankings:

$$\mathcal{L}_{out}(\theta_D) = \sum_i \sum_{j>i} \text{RK} [\eta'_{\xi_i}, \eta'_{\xi_j}; \mathbb{I}[\eta_{\xi_i} > \eta_{\xi_j}]], \quad (13)$$

where $\mathbb{I}[\eta_{\xi_i} > \eta_{\xi_j}]$ is 1 if $\eta_{\xi_i} > \eta_{\xi_j}$ and otherwise is -1 . RK is defined as a revised version of the widely-used margin ranking loss with margin as 0:

$$\text{RK} [\eta'_{\xi_i}; \eta'_{\xi_j}, \eta_{\xi_i}, \eta_{\xi_j}] = \begin{cases} \max(0, -\mathbb{I}[\eta_{\xi_i} > \eta_{\xi_j}](\eta'_{\xi_i} - \eta'_{\xi_j})), & |\eta'_{\xi_i} - \eta'_{\xi_j}| > \epsilon \\ \max(0, \frac{1}{4\epsilon}(\mathbb{I}[\eta_{\xi_i} > \eta_{\xi_j}](\eta'_{\xi_i} - \eta'_{\xi_j}) - \epsilon)^2), & |\eta'_{\xi_i} - \eta'_{\xi_j}| \leq \epsilon \end{cases} \quad (14)$$

We revised the original margin ranking loss within a ϵ range around the point of $(\eta'(\xi_i) - \eta'(\xi_j)) = 0$ to make it Lipschitz smooth. If we adopt small enough ϵ , the functionality of the revised marginal ranking loss is close to the original one. In all the experiments, we use $\epsilon = 10^{-5}$.

5 Experiments

In this section, we conduct experiments on the implementation of CAIL in Sec. 4.3. We verify the efficacy of the CAIL in simulated and real-world environments. We report the results on various compositions of demonstrations with varying optimality. **The code is available on our website³**

We conduct experiments in four environments including two MuJoCo environments (Reacher and Ant) [29] in OpenAI Gym [7], one Franka Panda Arm⁴ simulation environment, and one real robot environment with a UR5e robot arm⁵. For each environment, we collect a mixture of optimal and non-optimal demonstrations with different optimality to show the efficacy of CAIL. We investigate the performance with respect to the optimality of demonstrations ranging from failures to near-optimal or optimal demonstrations. We provide the implementation details and more results on the sensitivity of the parameters, and visualize the learned confidence in the supplementary materials.

Source of Demonstrations. For MuJoCo environments, following the demonstration collecting method in [31], we train a reinforcement learning algorithm and select four intermediate policies as policies with varying optimality and the converged policy as the optimal policy, so that the demonstrations range from worse-than-random ones to near-optimal ones. We draw 20% of demonstrations from each policy. For the RL algorithm, we use SAC [16] for the Reacher environment and PPO [25] for the Ant environment. For the Franka Panda Arm simulation and the real robot environment with UR5e, we hand-craft demonstrations with optimality varying continuously from near-optimal ones to unsuccessful ones to approximate the demonstration collecting process from demonstrators with different levels of expertise. We label only 5% of the demonstrated trajectories with rankings since we target realistic settings where only a small number of rankings are available for the demonstrations.

Baselines. We compare CAIL with the most relevant works in our problem setting including: the state-of-the-art standard imitation learning algorithms: GAIL [18], AIRL [14], imitation learning from suboptimal demonstration methods including two confidence-based methods, 2IWIL and IC-GAIL [31], and three ranking-based methods, T-REX [8], D-REX [9], and SSRR [12]. GAIL and AIRL learn directly from the mixture of optimal and non-optimal demonstrations. T-REX needs demonstrations paired with rankings, so we provide the same number of rankings as our approach. For D-REX and SSRR, we further generate rankings by disturbing demonstrations as done in their papers. For 2IWIL and IC-GAIL—that need a subset of demonstrations labeled with confidence—we label the subset of ranked demonstrations with evenly-spaced confidence, *i.e.*, the highest expected return as confidence 1, and the lowest expected return as 0. This is a reasonable approximation of the confidence score with no prior knowledge available. For a fair comparison, we re-implement 2IWIL with AIRL as its backbone imitation learning method. For the RL algorithm in T-REX, D-REX, and SSRR, we also use PPO. DPS [19] requires interactively collecting demonstrations and the approach in Cao *et al.* [11] requires the ground truth reward of demonstrations, which are both not implementable under the assumptions in our setting, so we do not include them.

5.1 Results

Reacher and Ant. In the Reacher, the end effector of the arm is supposed to reach a final location. Figure 2(a) shows the optimal trajectories of the joint and the end effector in green, which illustrates the policy reaching the location with the minimum energy cost, and the trajectories with lower optimality in red and orange, where the agent just spins around the center and wastes energy without reaching the target. We collect 200 trajectories in total, where each trajectory has 50 interaction steps.

In Ant, the agent has four legs, each with two links and two joints. Its goal is to move in the x-axis direction as fast as possible. Figure 2(b) illustrates the demonstrated trajectories, where green shows the optimal one, and red shows suboptimal trajectories (darker colors show lower optimality). In

³<https://sites.google.com/view/cail>

⁴<https://www.franka.de>

⁵<https://www.universal-robots.com/products/ur5-robot>

optimal demonstrations, the agent moves quickly along the x-axis, while in suboptimal ones, it moves slowly to other directions. We collect trajectories with 200,000 interaction steps in total.

As shown in Figure 2(e) and 2(f), CAIL achieves the highest expected return compared to the other methods and experiences fast convergence. For Reacher, the p-value⁶ between CAIL and the closest baseline method, T-REX, is 5.4054×10^{-6} (statistically significant). For Ant, the p-value between CAIL and the closest baseline method, 2IWIL, is 0.1405. CAIL outperforms standard imitation learning methods, GAIL and AIRL, because CAIL selects more useful demonstrations, and avoids the negative influence of harmful demonstrations. We observe that 2IWIL and IC-GAIL do not perform well because neighboring demonstrations in a given ranking are not guaranteed to have the same distance in terms of confidence score and thus the evenly-spaced confidence values derived from rankings are likely not accurate. All the ranking-based methods do not perform well. For T-REX, the potential reason can be that the rankings of a subset of demonstrations are not enough to learn a generalizable reward function covering states. For D-REX and SSR, the automatically generated rankings can be incorrect since we also have unsuccessful demonstrations—which can at times be worse than random actions—and perturbing such demonstrations is not guaranteed to produce demonstrations that imply rankings.

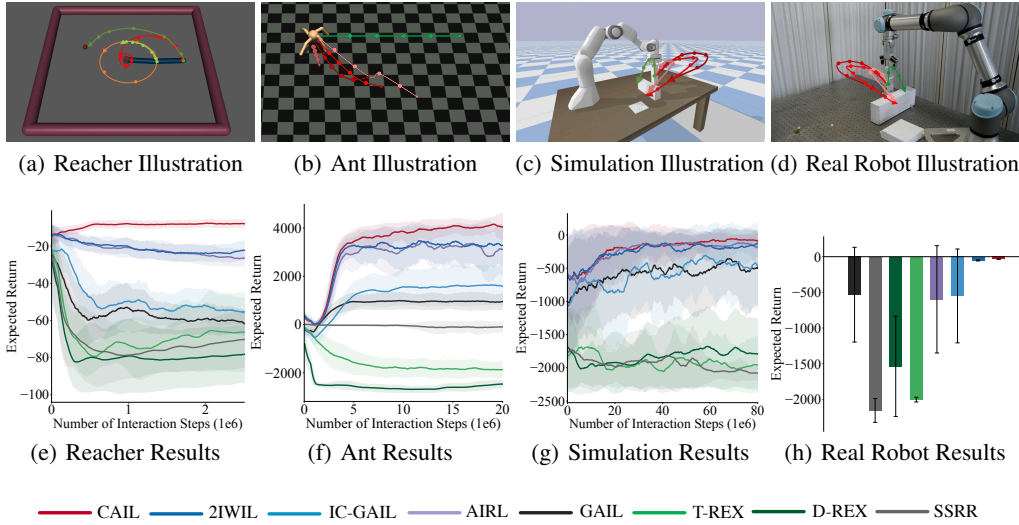


Figure 2: (a) Reacher, (b) Ant, (c) Simulated Panda Robot Arm, (d) Real UR5e Robot Arm. In (a-d), the green trajectories indicate the optimal demonstrations, while the red and orange trajectories indicate demonstrations with varying optimality. (e-g) The expected return with respect to the number of interaction steps. (h) The expected return of the converged policies for UR5e Robot Arm.

Robot Arm. We further conduct experiments in more realistic environments: a simulated Franka Panda Arm and a real UR5e robot arm. As shown in Figure 2(c) and 2(d), we design a task to let the robot arm pick up a bottle, avoid the obstacle, and put the bottle on a target platform. In the optimal demonstrations in green, the arm takes the shortest path to avoid the obstacle, and puts the bottle on the target, while in suboptimal ones in red (where, similar to before, the brightness of the trajectories indicates their optimality), the arm detours, does not reach the target, and even at times collides with the obstacle. The suboptimal demonstrations represent a wide range of optimality from near-optimal ones (small detour) to adversarial ones (colliding). We vary the initial position of the robot end-effector and the goal position within an initial area and goal area respectively. For both simulated and real robot environments, we collect trajectories with 200,000 interaction steps in total.

As shown in Figure 2(g) and 2(h), CAIL outperforms other methods in expected return in both the simulated and real robot environments. For the simulated robot arm environment, the p-value between CAIL and the closest baseline, 2IWIL, is 0.0974. For the real robot environment, the p-value between CAIL and the closest baseline, AIRL, is 0.0209 (statistically significant). In particular, in the real robot environment, CAIL achieves a low standard deviation while other methods especially AIRL, IC-GAIL, D-REX and GAIL suffer from an unstable performance. The results demonstrate that

⁶All p-values are computed by the student's t-test and the null hypothesis is the performance of CAIL is equal to or smaller than the baseline methods.

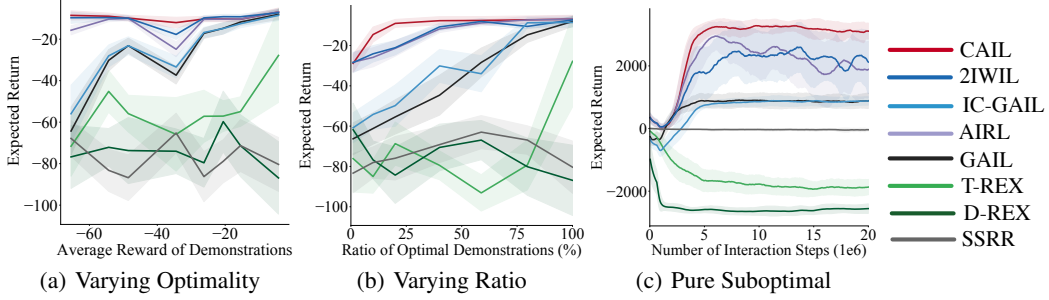


Figure 3: (a-b) The Expected Return with respect to different optimality of demonstrations in the Reacher environment, where the different optimality are created by varying the optimality of non-optimal demonstrations, and varying the ratio of optimal demonstrations. (c) Results for learning from only non-optimal demonstrations in the Ant environment.

CAIL can work stably in the real robot environment. We report the success rate—rate that the robot successfully reaches the target within the time limit without colliding with the obstacle—and videos of sample policy rollouts in the supplementary materials.

Demonstrations with Different Optimality. We show the performance of different methods with demonstrations at different levels of optimality in the Reacher environment. We fix 20% of the total demonstrations to be optimal and make the remaining 80% demonstration drawn from the same suboptimal policy. We vary the optimality of this policy to investigate the performance change with respect to different optimalities. Another way to obtain different optimality is to vary the ratio of optimal demonstrations. We show the results of both varying optimality in Figure 3(a) and 3(b) respectively. We observe that CAIL consistently outperforms or performs comparably to other methods with demonstrations at different optimality. Also, CAIL performs more stably while the baselines suffer from a performance drop at specific optimality levels.

Learning from Only Non-optimal Demonstrations. We verify that CAIL can also learn from solely non-optimal demonstrations without relying on any optimal demonstrations. We remove the optimal demonstrations in the Ant environment and use the remaining demonstrations to conduct imitation learning. As shown in Figure 3(c), CAIL still achieves the best performance among all the methods, which demonstrates that even with all demonstrations being non-optimal, CAIL still can learn useful knowledge from those demonstrations with higher expected return and induce a better policy. The highest p-value between CAIL and the closest baseline (2IWIL) is 0.0067, which indicates the performance gain is statistically significant. We observe that the performance of Airl first increases and then decreases. This is because even though the demonstrations are suboptimal, there are potentially optimal state-action transitions leading to the initial high performance. However, at this early training stage, the Airl model does not converge yet and the model parameters can still change rapidly. After training a sufficient number of steps, the Airl model observes both useful and less useful transitions and converges to the average return of all the demonstrations.

6 Conclusion

Summary. We propose a general learning framework, Confidence-Aware Imitation Learning, for imitation learning from demonstrations with varying optimality. We adopt standard imitation learning algorithms with their corresponding imitation loss (inner loss), and leverage an outer loss to evaluate the quality of the imitation learning model. We simultaneously learn a confidence score over the demonstrations using the outer loss and learn the policy through optimizing the inner loss over the confidence-reweighted distribution of demonstrations. Our framework is applicable to any imitation learning model with compatible choices of inner and outer losses. We provide theoretical guarantees on the convergence of CAIL and show that the learned policy outperforms baselines on various simulated and real-world environments under demonstrations with varying optimality.

Limitations and Future Work. Although we propose a flexible framework to address the problem of imitation learning from demonstrations with varying optimality, our work is limited in a few ways: To learn a well-performing policy, we still require that the dataset consists of demonstrations that encode useful knowledge for policy learning. We also require that the demonstrations and the imitation agent have the same dynamics. In the future, we plan to learn from demonstrations with more failures and relax the assumptions of the demonstrator and imitator having the same dynamics.

7 Acknowledgement

We would like to thank Tong Xiao for inspiring discussions about the backbone imitation learning algorithms and her help on the experiments. This work is funded by Tsinghua GuoQiang Research Institute, FLI grant RFP2-000, NSF Awards 1941722 and 1849952, and DARPA HiCoN project.

References

- [1] Pieter Abbeel and Andrew Y Ng. Apprenticeship learning via inverse reinforcement learning. In *Proceedings of the twenty-first international conference on Machine learning*, page 1, 2004.
- [2] Riad Akrou, Marc Schoenauer, and Michele Sebag. Preference-based policy learning. In *Joint European Conference on Machine Learning and Knowledge Discovery in Databases*, pages 12–27. Springer, 2011.
- [3] Brenna D Argall, Sonia Chernova, Manuela Veloso, and Brett Browning. A survey of robot learning from demonstration. *Robotics and autonomous systems*, 57(5):469–483, 2009.
- [4] Michael Bain and Claude Sammut. A framework for behavioural cloning. In *Machine Intelligence 15*, 1995.
- [5] Jonathan F Bard. *Practical bilevel optimization: algorithms and applications*, volume 30. Springer Science & Business Media, 2013.
- [6] Erdem Bıyık, Dylan P Losey, Malayandi Palan, Nicholas C Landolfi, Gleb Shevchuk, and Dorsa Sadigh. Learning reward functions from diverse sources of human feedback: Optimally integrating demonstrations and preferences. *arXiv preprint arXiv:2006.14091*, 2020.
- [7] Greg Brockman, Vicki Cheung, Ludwig Pettersson, Jonas Schneider, John Schulman, Jie Tang, and Wojciech Zaremba. Openai gym, 2016.
- [8] Daniel Brown, Wonjoon Goo, Prabhat Nagarajan, and Scott Niekum. Extrapolating beyond sub-optimal demonstrations via inverse reinforcement learning from observations. In *International Conference on Machine Learning*, pages 783–792. PMLR, 2019.
- [9] Daniel S Brown, Wonjoon Goo, and Scott Niekum. Better-than-demonstrator imitation learning via automatically-ranked demonstrations. In *Conference on Robot Learning*, pages 330–359. PMLR, 2020.
- [10] Benjamin Burchfiel, Carlo Tomasi, and Ronald Parr. Distance minimization for reward learning from scored trajectories. In *Proceedings of the AAAI Conference on Artificial Intelligence*, volume 30, 2016.
- [11] Zhangjie Cao and Dorsa Sadigh. Learning from imperfect demonstrations from agents with varying dynamics. *IEEE Robotics and Automation Letters (RA-L)*, 2021.
- [12] Letian Chen, Rohan Paleja, and Matthew Gombolay. Learning from suboptimal demonstration via self-supervised reward regression. In *Conference on Robot Learning*. PMLR, 2020.
- [13] Chelsea Finn, Paul Christiano, Pieter Abbeel, and Sergey Levine. A connection between generative adversarial networks, inverse reinforcement learning, and energy-based models. *arXiv preprint arXiv:1611.03852*, 2016.
- [14] Justin Fu, Katie Luo, and Sergey Levine. Learning robust rewards with adversarial inverse reinforcement learning. In *International Conference on Learning Representations*, 2018.
- [15] Ian Goodfellow, Jean Pouget-Abadie, Mehdi Mirza, Bing Xu, David Warde-Farley, Sherjil Ozair, Aaron Courville, and Yoshua Bengio. Generative adversarial nets. In *Advances in neural information processing systems*, pages 2672–2680, 2014.
- [16] Tuomas Haarnoja, Aurick Zhou, Pieter Abbeel, and Sergey Levine. Soft actor-critic: Off-policy maximum entropy deep reinforcement learning with a stochastic actor. In *International Conference on Machine Learning*, pages 1861–1870. PMLR, 2018.
- [17] Peter Henderson, Wei-Di Chang, Pierre-Luc Bacon, David Meger, Joelle Pineau, and Doina Precup. Optiongan: Learning joint reward-policy options using generative adversarial inverse reinforcement learning. In *Proceedings of the AAAI Conference on Artificial Intelligence*, volume 32, 2018.

- [18] Jonathan Ho and Stefano Ermon. Generative adversarial imitation learning. In *Advances in neural information processing systems*, pages 4565–4573, 2016.
- [19] Ellen R. Novoseller, Yibng Wei, Yanan Sui, Yisong Yue, and J. Burdick. Dueling posterior sampling for preference-based reinforcement learning. In *Uncertainty in Artificial Intelligence (UAI)*, 2020.
- [20] Adam Paszke, Sam Gross, Francisco Massa, Adam Lerer, James Bradbury, Gregory Chanan, Trevor Killeen, Zeming Lin, Natalia Gimelshein, Luca Antiga, et al. Pytorch: An imperative style, high-performance deep learning library. *arXiv preprint arXiv:1912.01703*, 2019.
- [21] Dean A Pomerleau. Efficient training of artificial neural networks for autonomous navigation. *Neural computation*, 3(1):88–97, 1991.
- [22] Deepak Ramachandran and Eyal Amir. Bayesian inverse reinforcement learning. In *IJCAI*, volume 7, pages 2586–2591, 2007.
- [23] Stéphane Ross, Geoffrey Gordon, and Drew Bagnell. A reduction of imitation learning and structured prediction to no-regret online learning. In *Proceedings of the fourteenth international conference on artificial intelligence and statistics*, pages 627–635, 2011.
- [24] Stefan Schaal. Is imitation learning the route to humanoid robots? *Trends in cognitive sciences*, 3(6):233–242, 1999.
- [25] John Schulman, Filip Wolski, Prafulla Dhariwal, Alec Radford, and Oleg Klimov. Proximal policy optimization algorithms. *arXiv preprint arXiv:1707.06347*, 2017.
- [26] Hiroaki Sugiyama, Toyomi Meguro, and Yasuhiro Minami. Preference-learning based inverse reinforcement learning for dialog control. In *Thirteenth Annual Conference of the International Speech Communication Association*, 2012.
- [27] Voot Tangkaratt, Nontawat Charoenphakdee, and Masashi Sugiyama. Robust imitation learning from noisy demonstrations. *arXiv preprint arXiv:2010.10181*, 2020.
- [28] Voot Tangkaratt, Bo Han, Mohammad Emtiyaz Khan, and Masashi Sugiyama. Variational imitation learning with diverse-quality demonstrations. In Hal Daumé III and Aarti Singh, editors, *Proceedings of the 37th International Conference on Machine Learning*, volume 119 of *Proceedings of Machine Learning Research*, pages 9407–9417, Virtual, 13–18 Jul 2020. PMLR.
- [29] Emanuel Todorov, Tom Erez, and Yuval Tassa. Mujoco: A physics engine for model-based control. In *2012 IEEE/RSJ International Conference on Intelligent Robots and Systems*, pages 5026–5033. IEEE, 2012.
- [30] Christian Wirth, Johannes Fürtkranz, and Gerhard Neumann. Model-free preference-based reinforcement learning. In *Proceedings of the AAAI Conference on Artificial Intelligence*, volume 30, 2016.
- [31] Yueh-Hua Wu, Nontawat Charoenphakdee, Han Bao, Voot Tangkaratt, and Masashi Sugiyama. Imitation learning from imperfect demonstration. In *International Conference on Machine Learning*, pages 6818–6827, 2019.
- [32] Junzhe Zhang, Daniel Kumor, and Elias Bareinboim. Causal imitation learning with unobserved confounders. *Advances in neural information processing systems*, 33, 2020.
- [33] Brian D Ziebart, Andrew L Maas, J Andrew Bagnell, and Anind K Dey. Maximum entropy inverse reinforcement learning. In *Aaai*, volume 8, pages 1433–1438. Chicago, IL, USA, 2008.

A Proofs

In this section, we provide the proofs of the theorems in Section 4.2 of the main text.

A.1 Preliminaries

Definition 1. (*Lipschitz-smooth*) Function $f(x) : \mathbb{R}^d \rightarrow \mathbb{R}$ is *Lipschitz-smooth* with constant L if

$$\|\nabla f(x) - \nabla f(y)\| \leq L\|x - y\|, \quad \forall x, y \in \mathbb{R}^d \quad (15)$$

Lemma 1. If function $f(x)$ is *Lipschitz-smooth* with constant L , then the following inequality holds:

$$(\nabla f(x) - \nabla f(y))^T (x - y) \leq L\|x - y\|^2 \quad (16)$$

Proof. The proof is straight forward that

$$\begin{aligned} & (\nabla f(x) - \nabla f(y))^T (x - y) \\ & \leq \|\nabla f(x) - \nabla f(y)\| \cdot \|x - y\| \\ & \leq L\|x - y\|^2 \end{aligned} \quad (17)$$

The first equation follows from the Cauchy-Schwarz inequality, and the second inequality comes from the definition of Lipschitz-smooth. \square

Lemma 2. If function $f(x)$ is *Lipschitz-smooth* with constant L , then the following inequality holds:

$$f(y) \leq f(x) + \nabla f(x)^T (y - x) + \frac{L}{2}\|y - x\|^2, \quad \forall x, y \quad (18)$$

Proof. Define $g(t) = f(x + t(y - x))$. If $f(x)$ is Lipschitz-smooth with constant L , then from Lemma 1, we have

$$\begin{aligned} & g'(t) - g'(0) \\ & = (\nabla f(x + t(y - x)) - \nabla f(x))^T (y - x) \\ & = \frac{1}{t} (\nabla f(x + t(y - x)) - \nabla f(x))^T ((x + t(y - x)) - x) \\ & \leq \frac{L}{t} \|t(y - x)\|^2 = tL\|y - x\|^2 \end{aligned} \quad (19)$$

We then integrate this equation from $t = 0$ to $t = 1$:

$$\begin{aligned} f(y) &= g(1) = g(0) + \int_0^1 g'(t) dt \\ &\leq g(0) + \int_0^1 g'(0) dt + \int_0^1 tL\|y - x\|^2 dt \\ &= g(0) + g'(0) + \frac{L}{2}\|y - x\|^2 \\ &= f(x) + \nabla f(x)^T (y - x) + \frac{L}{2}\|y - x\|^2 \end{aligned} \quad (20)$$

\square

A.2 Proof of Theoretical Results

In this section, we provide the proofs of the theorems proposed in this paper. First, we provide the proof of Theorem 1 in the main text.

Theorem 1. (*Convergence*) Suppose the outer loss \mathcal{L}_{out} is Lipschitz-smooth with constant L , the inequality

$$\nabla_{\theta} \mathcal{L}_{out}(\theta_{\tau+1})^\top \nabla_{\theta} \mathcal{L}_{in}(\theta_{\tau}, \beta_{\tau+1}) \geq C \|\nabla_{\theta} \mathcal{L}_{in}(\theta_{\tau}, \beta_{\tau+1})\|^2 \quad (21)$$

holds for a constant $C \geq 0$ in every step τ^7 , and the learning rate satisfies $\mu \leq \frac{2C}{L}$, then the outer loss decreases along with each iteration: $\mathcal{L}_{\text{out}}(\theta_{\tau+1}) \leq \mathcal{L}_{\text{out}}(\theta_\tau)$, and the equality holds if $\nabla_\beta \mathcal{L}_{\text{out}}(\theta_\tau) = 0$ or $\theta_{\tau+1} = \theta_\tau$.

Proof. Since \mathcal{L}_{out} is Lipschitz-smooth, following Lemma 2, we have

$$\begin{aligned}
& \mathcal{L}_{\text{out}}(\theta_{\tau+1}) - \mathcal{L}_{\text{out}}(\theta_\tau) \\
& \leq \nabla_\theta \mathcal{L}_{\text{out}}(\theta_\tau)^T (\theta_{\tau+1} - \theta_\tau) + \frac{L}{2} \|(\theta_{\tau+1} - \theta_\tau)\|^2 \\
& = -\mu \nabla_\theta \mathcal{L}_{\text{out}}(\theta_{\tau+1})^T \nabla_\theta \mathcal{L}_{\text{in}}(\theta_\tau, \beta_{\tau+1}) \\
& \quad + \frac{L}{2} \mu^2 \|\nabla_\theta \mathcal{L}_{\text{in}}(\theta_\tau, \beta_{\tau+1})\|^2 \\
& \leq -\left(\mu C - \frac{L}{2} \mu^2\right) \|\nabla_\theta \mathcal{L}_{\text{in}}(\theta_\tau, \beta_{\tau+1})\|^2 \\
& \leq 0
\end{aligned} \tag{22}$$

The first inequality comes from Lemma 2, and the second inequality holds because we update θ_τ to $\theta_{\tau+1}$ only when $\nabla_\theta \mathcal{L}_{\text{out}}(\theta_{\tau+1})^T \nabla_\theta \mathcal{L}_{\text{in}}(\theta_\tau, \beta_{\tau+1}) \geq C \|\nabla_\theta \mathcal{L}_{\text{in}}(\theta_\tau, \beta_{\tau+1})\|^2$ holds, otherwise $\theta_{\tau+1} = \theta_\tau$ so $\mathcal{L}_{\text{out}}(\theta_{\tau+1}) = \mathcal{L}_{\text{out}}(\theta_\tau)$. The third inequality holds because we choose the learning rate to satisfy $\mu \leq \frac{2C}{L}$.

Then if $\nabla_\theta \mathcal{L}_{\text{out}}(\theta_\tau) = 0$, and if Eqn. (21) is satisfied, we have $\nabla_\theta \mathcal{L}_{\text{in}}(\theta_\tau, \beta_{\tau+1}) = 0$. Following the updating rule of α in Eqn. (10), we can derive $\theta_{\tau+1} = \theta_\tau$, so $\mathcal{L}_{\text{out}}(\theta_{\tau+1}) = \mathcal{L}_{\text{out}}(\theta_\tau)$. Besides, if Eqn. (11) is not satisfied, we also have $\theta_{\tau+1} = \theta_\tau$, and thus $\mathcal{L}_{\text{out}}(\theta_{\tau+1}) = \mathcal{L}_{\text{out}}(\theta_\tau)$. \square

We now provide the proof of Theorem 2 on convergence rate of the algorithm.

Theorem 2. (Convergence Rate) Under the assumptions in Theorem 1, let

$$g(\theta, \beta) = \theta - \mu \nabla_\theta \mathcal{L}_{\text{in}}(s, a; \theta, \beta). \tag{23}$$

We assume that $\mathcal{L}_{\text{out}}(g(\theta, \beta))$ is Lipschitz-smooth w.r.t. β with constant L_1 , \mathcal{L}_{in} and \mathcal{L}_{out} have σ -bounded gradients, and the norm of $\nabla_\beta \nabla_\theta \mathcal{L}_{\text{in}}(\theta; \beta)$ is bounded by σ_1 . L is the Lipschitz-smooth constant for \mathcal{L}_{out} w.r.t. $g(\theta, \beta)$ as shown in Theorem 1. Consider the total training steps as T , we set $\alpha = \frac{C_1}{\sqrt{T}}$, for some constant C_1 where $0 < C_1 \leq \frac{2}{L_1}$ and $\mu = \frac{C_2}{T}$ for some constant C_2 . CAIL can achieve:

$$\min_{1 \leq \tau \leq T} \mathbb{E}[\|\nabla_\beta \mathcal{L}_{\text{out}}(\theta_\tau)\|^2] \leq O\left(\frac{1}{\sqrt{T}}\right). \tag{24}$$

Proof. According to the update rule of θ , we have

$$\begin{aligned}
& \mathcal{L}_{\text{out}}(\theta_{\tau+1}) - \mathcal{L}_{\text{out}}(\theta_\tau) \\
& = \mathcal{L}_{\text{out}}(\theta_\tau - \mu \nabla_\theta \mathcal{L}_{\text{in}}(\theta_\tau, \beta_{\tau+1})) \\
& \quad - \mathcal{L}_{\text{out}}(\theta_{\tau-1} - \mu \nabla_\theta \mathcal{L}_{\text{in}}(\theta_{\tau-1}, \beta_\tau)) \\
& = \{\mathcal{L}_{\text{out}}(\theta_\tau - \mu \nabla_\theta \mathcal{L}_{\text{in}}(\theta_\tau, \beta_{\tau+1})) \\
& \quad - \mathcal{L}_{\text{out}}(\theta_{\tau-1} - \mu \nabla_\theta \mathcal{L}_{\text{in}}(\theta_{\tau-1}, \beta_{\tau+1}))\} \\
& \quad + \{\mathcal{L}_{\text{out}}(\theta_{\tau-1} - \mu \nabla_\theta \mathcal{L}_{\text{in}}(\theta_{\tau-1}, \beta_{\tau+1})) \\
& \quad - \mathcal{L}_{\text{out}}(\theta_{\tau-1} - \mu \nabla_\theta \mathcal{L}_{\text{in}}(\theta_{\tau-1}, \beta_\tau))\} \\
& = \{\mathcal{L}_{\text{out}}(g(\theta_\tau, \beta_{\tau+1})) - \mathcal{L}_{\text{out}}(g(\theta_{\tau-1}, \beta_{\tau+1}))\} \\
& \quad + \{\mathcal{L}_{\text{out}}(g(\theta_{\tau-1}, \beta_{\tau+1})) - \mathcal{L}_{\text{out}}(g(\theta_{\tau-1}, \beta_\tau))\}
\end{aligned} \tag{25}$$

We remove (s, a) in the \mathcal{L}_{in} for notation convenience. For the first term,

$$\begin{aligned}
& \mathcal{L}_{\text{out}}(g(\theta_\tau, \beta_{\tau+1})) - \mathcal{L}_{\text{out}}(g(\theta_{\tau-1}, \beta_{\tau+1})) \\
& \leq \nabla \mathcal{L}_{\text{out}}(g(\theta_{\tau-1}, \beta_{\tau+1}))^T \Delta g + \frac{L}{2} \|\Delta g\|^2
\end{aligned} \tag{26}$$

⁷We remove (s, a) in \mathcal{L}_{in} for notation simplicity.

where

$$\begin{aligned}
\Delta g &= g(\theta_\tau, \beta_{\tau+1}) - g(\theta_{\tau-1}, \beta_{\tau+1}) \\
&= [\theta_\tau - \mu \nabla_\theta \mathcal{L}_{\text{in}}(\theta_\tau, \beta_{\tau+1})] \\
&\quad - [\theta_{\tau-1} - \mu \nabla_\theta \mathcal{L}_{\text{in}}(\theta_{\tau-1}, \beta_{\tau+1})] \\
&= -\mu [\nabla_\theta \mathcal{L}_{\text{in}}(\theta_\tau, \beta_{\tau+1}) + \nabla_\theta \mathcal{L}_{\text{in}}(\theta_{\tau-1}, \beta_\tau) \\
&\quad - \nabla_\theta \mathcal{L}_{\text{in}}(\theta_{\tau-1}, \beta_{\tau+1})]
\end{aligned} \tag{27}$$

Since \mathcal{L}_{in} has σ -bounded gradients, we take the norm on both sides, and use the triangle inequality, so

$$\|\Delta g\| \leq 3\mu\sigma \tag{28}$$

Substitute this into Eqn. (26), we have

$$\begin{aligned}
&\mathcal{L}_{\text{out}}(g(\theta_\tau, \beta_{\tau+1})) - \mathcal{L}_{\text{out}}(g(\theta_{\tau-1}, \beta_{\tau+1})) \\
&\leq 3\mu\sigma^2 + \frac{9}{2}L\mu^2\sigma^2
\end{aligned} \tag{29}$$

And for the second term,

$$\begin{aligned}
&\mathcal{L}_{\text{out}}(g(\theta_{\tau-1}, \beta_{\tau+1})) - \mathcal{L}_{\text{out}}(g(\theta_{\tau-1}, \beta_\tau)) \\
&\leq \nabla_\beta \mathcal{L}_{\text{out}}(g(\theta_{\tau-1}, \beta_\tau))^T (\beta_{\tau+1} - \beta_\tau) + \frac{L_1}{2} \|\beta_{\tau+1} - \beta_\tau\|^2 \\
&= -\alpha \nabla_\beta \mathcal{L}_{\text{out}}(g(\theta_{\tau-1}, \beta_\tau))^T \nabla_\beta \mathcal{L}_{\text{out}}(g(\theta_\tau, \beta_\tau)) \\
&\quad + \frac{L_1\alpha^2}{2} \|\nabla_\beta \mathcal{L}_{\text{out}}(g(\theta_\tau, \beta_\tau))\|^2 \\
&= -(\alpha - \frac{L_1\alpha^2}{2}) \|\nabla_\beta \mathcal{L}_{\text{out}}(g(\theta_\tau, \beta_\tau))\|^2 \\
&\quad + \alpha (\nabla_\beta \mathcal{L}_{\text{out}}(g(\theta_\tau, \beta_\tau)) - \nabla_\beta \mathcal{L}_{\text{out}}(g(\theta_{\tau-1}, \beta_\tau)))^T \nabla_\beta \mathcal{L}_{\text{out}}(g(\theta_\tau, \beta_\tau))
\end{aligned} \tag{30}$$

Since $\nabla_\beta \nabla_\theta \mathcal{L}_{\text{in}}(\theta, \beta)$ is bounded by σ_1 and \mathcal{L} has σ -bounded gradients, then

$$\begin{aligned}
&\nabla_\beta \mathcal{L}_{\text{out}}(g(\theta, \beta)) \\
&= \nabla_\beta g(\theta, \beta)^T \nabla_g \mathcal{L}_{\text{out}}(g(\theta, \beta)) \\
&= -\mu \nabla_\beta \nabla_\theta \mathcal{L}_{\text{in}}(\theta, \beta)^T \nabla_g \mathcal{L}_{\text{out}}(g(\theta, \beta)) \\
&\leq \mu\sigma\sigma_1
\end{aligned} \tag{31}$$

So

$$\begin{aligned}
&\mathcal{L}_{\text{out}}(g(\theta_{\tau-1}, \beta_{\tau+1})) - \mathcal{L}_{\text{out}}(g(\theta_{\tau-1}, \beta_\tau)) \\
&\leq -(\alpha - \frac{L_1\alpha^2}{2}) \|\nabla_\beta \mathcal{L}_{\text{out}}(g(\theta_\tau, \beta_\tau))\|^2 \\
&\quad + 2\alpha\mu\sigma\sigma_1
\end{aligned} \tag{32}$$

Combining the two parts, we can derive that

$$\begin{aligned}
&\mathcal{L}_{\text{out}}(\theta_{\tau+1}) - \mathcal{L}_{\text{out}}(\theta_\tau) \\
&\leq -(\alpha - \frac{L_1\alpha^2}{2}) \|\nabla_\beta \mathcal{L}_{\text{out}}(g(\theta_\tau, \beta_\tau))\|^2 \\
&\quad + 3\mu\sigma^2 + \frac{9}{2}L\mu^2\sigma^2 + 2\alpha\mu\sigma\sigma_1
\end{aligned} \tag{33}$$

Summing up both sides from $\tau = 1$ to T , and rearranging the terms, we can derive that

$$\begin{aligned}
&\sum_{\tau=1}^T (\alpha - \frac{L_1\alpha^2}{2}) \|\nabla_\beta \mathcal{L}_{\text{out}}(\theta_\tau)\|^2 \\
&\leq \mathcal{L}_{\text{out}}(\theta_1) - \mathcal{L}_{\text{out}}(\theta_{T+1}) + T \left(3\mu\sigma^2 + \frac{9}{2}L\mu^2\sigma^2 + 2\alpha\mu\sigma\sigma_1 \right)
\end{aligned} \tag{34}$$

Since $\alpha - \frac{L_1\alpha^2}{2} \geq 0$, we have

$$\begin{aligned}
& \min_{\tau} \mathbb{E}[\|\nabla_{\beta} \mathcal{L}_{\text{out}}(\theta_t)\|^2] \\
& \leq \frac{\sum_{\tau=1}^T (\alpha - \frac{L_1\alpha^2}{2}) \|\nabla_{\beta} \mathcal{L}_{\text{out}}(\theta_t)\|^2}{T(\alpha - \frac{L_1\alpha^2}{2})} \\
& \leq \frac{1}{T\alpha(1 - \frac{L_1\alpha}{2})} [\mathcal{L}_{\text{out}}(\theta_1) - \mathcal{L}_{\text{out}}(\theta_{T+1}) \\
& \quad + T \left(3\mu\sigma^2 + \frac{9}{2}L\mu^2\sigma^2 + 2\alpha\mu\sigma\sigma_1 \right)] \\
& \leq \frac{1}{\alpha\sqrt{T}(\sqrt{T}-1)} [\mathcal{L}_{\text{out}}(\theta_1) - \mathcal{L}_{\text{out}}(\theta_{T+1}) \\
& \quad + T \left(3\mu\sigma^2 + \frac{9}{2}L\mu^2\sigma^2 + 2\alpha\mu\sigma\sigma_1 \right)] \tag{35} \\
& = \frac{\mathcal{L}_{\text{out}}(\theta_1) - \mathcal{L}_{\text{out}}(\theta_{T+1})}{\alpha\sqrt{T}(\sqrt{T}-1)} + \frac{\sigma\mu\sqrt{T}}{\alpha(\sqrt{T}-1)} \left(3\sigma + \frac{9}{2}L\mu\sigma + 2\alpha\sigma_1 \right) \\
& = \frac{\mathcal{L}_{\text{out}}(\theta_1) - \mathcal{L}_{\text{out}}(\theta_{T+1})}{C_1(\sqrt{T}-1)} + \frac{\sigma C_2}{C_1(\sqrt{T}-1)} \left(3\sigma + \frac{9}{2}L\mu\sigma + 2\alpha\sigma_1 \right) \\
& = O\left(\frac{1}{\sqrt{T}}\right)
\end{aligned}$$

The second inequality holds since $1 - \frac{L_1\alpha}{2} \geq 1 - \frac{1}{\sqrt{T}}$. \square

Theorem 3. *RK in Eqn. (14) in the main text is Lipschitz.*

Proof. We consider the case where $\eta_{\xi_i} > \eta_{\xi_j}$. The case for $\eta_{\xi_i} \leq \eta_{\xi_j}$ can be demonstrated similarly. We prove that RK is Lipschitz by definition. Let $z = \xi'_i - \xi'_j$, the derivative of RK is

$$\nabla RK_z = \begin{cases} 0 & z > \epsilon, \\ \frac{1}{2\epsilon}(z - \epsilon) & -\epsilon \leq z \leq \epsilon, \\ -1 & z < -\epsilon \end{cases}$$

Thus, the second-order derivative of RK satisfies that $|\nabla(\nabla RK_z)_z| \leq \frac{1}{2\epsilon}$. If we take $L > \frac{1}{2\epsilon}$, then $\forall z_1, z_2, |\nabla(z_1) - \nabla(z_2)| < L|z_1 - z_2|$. This proves that RK is Lipschitz smooth. \square

B Experiments

In this section, we provide additional experimental details and results.

B.1 Experimental Details

We first go over the implementation details. We will then describe the environments and details of running experiments including train/validation/test splits, the number of evaluation runs, the average time for each run, and the used computing infrastructure.

B.1.1 Implementation Details

We implement CAIL based on a PPO-based AIRL. The actor and the critic are neural networks with two hidden layers with size 64 and Tanh as the activation function, and the discriminator is a neural network with two hidden layers with size 100 and ReLU as the activation function. We use ADAM to update the imitation learning model and Stochastic Gradient Descent method (SGD) to update the confidence. We implement our method in the PyTorch framework [20]. We train each algorithm 10 times with different random seeds, and record how the expected return and the standard deviation varies during training. While testing the return, we run the algorithm for 100 episodes.

While implementing Eqn. (11), we normalize β so that their mean value is 1, i.e. for the first part of Eqn. (11), we use $\sum_{(s,a) \in \Xi} \left(-\frac{n\beta(s,a)}{\sum_{(s,a) \in \Xi} \beta(s,a)} \right) \log(D(s,a))$, where n is the number of state-action pairs in Ξ . All the experiments in all environments are run on one Intel(R) Xeon(R) Gold 6244 CPU @ 3.60GHz with 10G memory.

B.1.2 Environment

Reacher. In the Reacher environment, the agent is an arm with two links and one joint, and the end effector of the arm is supposed to reach a final location. Each step, the agent is penalized for the energy cost and the distance to the target.

We collect 200 trajectories in total for training, where each trajectory has 50 interaction steps. 5% of the trajectories are annotated with rankings. We collect 5 trajectories for testing. We run the experiment for 5 runs and compute the mean and the standard deviation of the expected return. The average time for each run is 1,291s.

Ant. In the Ant environment, the agent is an ant with four legs and each leg has two links and two joints. Its goal is to move forward in the x-axis direction as fast as possible. Each step, the agent is rewarded for moving fast in the x-axis direction without falling down, while it is penalized for the energy cost. If the ant fails to stand, the trajectory will be terminated.

We collect 200 trajectories in total for training, where each trajectory has at most 1000 interaction steps. 5% of the trajectories are annotated with rankings. We collect 5 trajectories for testing. We run the experiment for 5 runs and compute the mean and the standard deviation of the expected return. The average time for each run is 17,140s.

Simulated Robot Arm. In this environment, there is a Franka Panda Arm that is supposed to pick up a bottle, avoid the obstacle, and put the bottle on a target platform. Each step, the agent is penalized for the energy cost and the distance to the target. If the agent drops the bottle or hits the target, it will receive a large negative reward and the trajectory will be terminated. If the agent succeeds to make the bottle stand on the target, the trajectory will be terminated too, so that the arm will no longer receive penalization. The reachable region of the arm is $[0.20, 0.80]$ in x-axis, and $[-0.35, 0.35]$ in y-axis. The initial position of the bottle is sampled in $[0.68, 0.72] \times [-0.05, 0]$ and the initial position of the target is sampled in $[0.28, 0.32] \times [-0.32, -0.28]$. The action space is the velocity of the end-effector, and the maximum velocity is 1 in each direction.

We collect 200 trajectories in total for training, where each trajectory has at most 2000 interaction steps. 5% of the trajectories are annotated with rankings. We collect 5 trajectories for testing. We run the experiment for 5 runs and compute the mean and the standard deviation of the expected return. The average time for each run is 44,731s.

Real Robot Arm. In this environment, we use a real UR5e robot arm in a similar settings as the simulation environment.

We collect 200 trajectories in total for training, where each trajectory has at most 2000 interaction steps. 5% of the trajectories are annotated with rankings. We collect 5 trajectories for testing. We run the experiment for 5 runs and compute the mean and the standard deviation of the expected return. The average time for each run is 141,699s.

B.1.3 Evaluation Metrics

To evaluate the proposed CAIL and other methods, we use the expected return for all the environments, which is the discounted cumulative reward of a trajectory. For the Reacher and the Ant environments, we use the reward function in their original implementation in Gym⁸. For the Simulated Robot Arm and the Real Robot Arm environments, we define a reward as follows: Assume that the action of the robot arm (the velocity of the end-effector) is a , the distance between the bottle and the target is d , the distance between the bottle's initial position and the target is d_{init} , then at each step, the robot will receive a reward of $-\frac{0.02a}{d_{\text{init}}^2} - 0.05d$. If the robot drops the bottle or the obstacle is moved, the robot will receive a reward of -2000 and the trajectory will be terminated. In the robot arm environments

⁸<https://github.com/openai/gym>

(both simulated and real), we also use the success rate as another metric to evaluate the rate that the robot arm successfully moves the bottle to the goal area without colliding with the obstacle.

B.2 Results

Table 1: The converged expected return of all the methods in Mujoco Reacher and Ant, Simulated Franka Panda Robot Arm, and the Real UR5e Robot Arm environments. We provide numerical results for a clearer comparison.

Method	Reacher	Ant	Simulated Robot	Real Robot
CAIL	-7.816 \pm 1.518	3825.644 \pm 940.279	-62.946 \pm 50.644	-34.330 \pm 1.242
2IWIL	-23.055 \pm 3.803	3473.852 \pm 271.696	-120.622 \pm 122.787	-52.445 \pm 7.182
IC-GAIL	-55.355 \pm 5.046	1525.671 \pm 747.884	-349.511 \pm 342.597	-550.235 \pm 657.838
AIRL	-25.922 \pm 2.337	3016.134 \pm 1028.894	-236.953 \pm 230.495	-597.819 \pm 752.149
GAIL	-60.858 \pm 3.299	998.231 \pm 387.825	-527.604 \pm 452.379	-532.854 \pm 664.415
T-REX	-66.371 \pm 21.295	-1867.930 \pm 318.339	-1933.944 \pm 380.834	-2003.672 \pm 32.771
D-REX	-78.102 \pm 14.918	-2467.779 \pm 135.175	-1817.239 \pm 481.672	-1538.100 \pm 703.266
SSRR	-70.044 \pm 14.735	-105.346 \pm 210.837	-2077.616 \pm 58.764	-2154.214 \pm 168.086
Oracle	-4.312	4787.233	-35.362	-31.056

Numerical Comparison. We provide the numerical comparison of CAIL and the baseline methods in Table 1. The results correspond to the results in Fig. 2 in the main text. We can observe that CAIL outperforms all the baseline methods in all the environments and the margin between CAIL and the best-performing policy is much closer than the margin between baseline methods and the best-performing policy.

Table 2: Success rate (%) among 100 trials of all the methods in the simulated and real robot environments.

Method	CAIL	2IWIL	IC-GAIL	AIRL	GAIL	T-REX	D-REX	SSRR
Simulated Robot	100	100	81	87	31	0	0	0
Real Robot	100	83	7	33	20	0	0	0

Success Rate. We report the success rate among 100 trials of different methods in Table 2. We observe that for both simulated and real robot environments, CAIL achieves the highest success rate. Though 2IWIL also achieves a high success rate; however, it induces trajectories with longer detour and thus has lower expected return.

Table 3: The performance with respect to the size of the ranking dataset.

Label Ratio	1%	2%	5%	10%	20%	50%	100%
2IWIL	-33.5 \pm 4.9	-34.4 \pm 3.2	-23.3 \pm 4.1	-27.7 \pm 6.7	-24.5 \pm 3.0	-30.0 \pm 2.7	-25.2 \pm 6.9
IC-GAIL	-56.4 \pm 10.1	-53.7 \pm 4.0	-61.0 \pm 5.0	-54.1 \pm 6.0	-58.8 \pm 3.4	-44.6 \pm 8.3	-57.1 \pm 3.7
T-REX	-83.7 \pm 18.6	-85.8 \pm 15.3	-82.3 \pm 10.2	-73.2 \pm 21.6	-91.8 \pm 15.4	-38.6 \pm 35.8	-27.2 \pm 37.2
CAIL	-8.0 \pm 2.4	-8.7 \pm 3.6	-7.3 \pm 2.0	-8.1 \pm 2.9	-7.1 \pm 1.7	-7.5 \pm 2.3	-7.8 \pm 3.0

Ablating the size of ranking dataset We provide results of CAIL and the compared methods including 2IWIL, IC-GAIL, and T-REX with varying levels of supervision. We do not include GAIL, AIRL, D-REX, and SSRR in this ablation since they do not require any supervision. We conduct experiments in the Reacher environment, and vary the ratio of demonstrations labeled with ranking. The agents are provided with 200 trajectories, and the ratios of labeled demonstrations are 1%, 2%, 5%, 10%, 20%, 50%, 100%. The average trajectory rewards and the standard deviations are shown in the Table 3. CAIL outperforms all the other methods with a large gap in all settings, even in the setting with only 1% labeled demonstrations, i.e., only two trajectories are labeled, which is the minimum label we can have for ranking. 2IWIL and IC-GAIL, however, do not perform well, and there is no clear increase of performance as the label ratio increases. This is because what they need is labeled confidence, which is a much stronger type of supervision than ranking. The confidence cannot be accurately recovered when only given rankings. T-REX does not perform well either, but

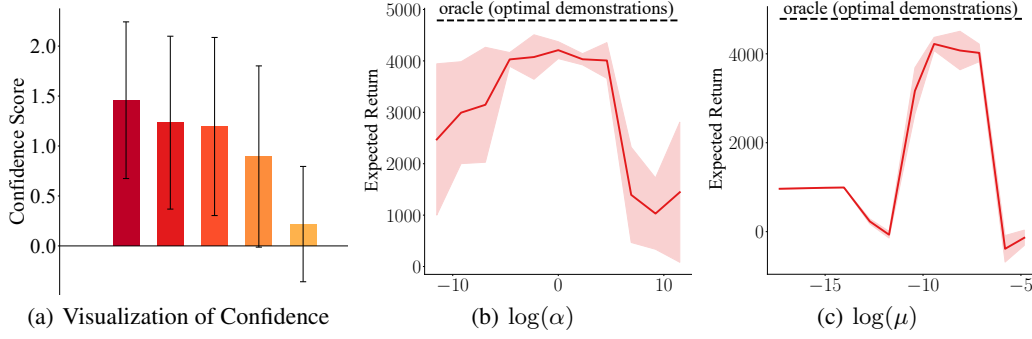


Figure 4: (a) The visualization of confidence for demonstrations drawn from policies with different optimality. There are 5 policies with different optimality, where the darker color means the policy has higher expected return. (b-c) The expected return with varying hyper-parameters α and μ .

it is getting better as the ratio of labels increases. This experimentally proves that T-REX needs much more data than CAIL to learn a reward function and CAIL can use the demonstrations more efficiently.

Visualization of the Confidence In our experiments, we have 5 sets of demonstrations collected from 5 different policies, where each set of demonstrations has different average returns. So we can learn different average confidence values for each different set of demonstrations. The larger the average return, the larger the average confidence. In our framework, we learn a confidence for each state-action pair. We visualize the un-normalized confidence learned by CAIL of these 5 set of demonstrations in Fig. 4(a), where the darker color means the demonstrations have higher expected returns. We observe that the darker color bar has higher confidence, which indicates that CAIL-learned confidence matches the optimality of the demonstrations.

Hyper-parameter Sensitivity. We investigate the sensitivity of hyper-parameters including the two learning rates α and μ . We aim to demonstrate two points: (1) The proposed approach can work stably with the hyper-parameters falling into a specific range; (2) If the hyper-parameters are too large or too small, the performance can drop, which means that tuning the two hyper-parameters are necessary for the performance of our algorithm. We conduct experiments in the Ant environment. As shown in Figure 4(b) and 4(c), the proposed approach work stably with α in the range $[10^{-3}, 100.0]$, and with μ in the range $[3 \times 10^{-5}, 3 \times 10^{-4}]$. When α and μ are too large or too small, the performance drops. The observations demonstrate the two points introduced above.

Videos for Real Robot. We show the videos of experiments in the real UR5e robot arm environment in the file 'robot_video.mp4' in the supplementary materials.